Accurate Information vs. Looks Good: Scientific vs. Preferred Rendering

John McCann, McCann Imaging; Belmont, MA 02478, USA
Vassilios Vonikakis, Advanced Digital Sciences Center (ADSC); Singapore

Abstract

Scientists use digital camera data as the input to their analysis of image processing algorithms. In this paper we measured the "engineered color errors" introduced by digital camera color processing. Camera manufactures build their color management systems using the sRGB design standard. Although that sRGB is a guideline in the beginning, the final firmware shows certain liberties taken to make the best preferred rendering of scenes. The ensemble of algorithms that perform the color balance, color enhancement, tone scale, and post-LUT for display and printing, create large discrepancies between the sRGB measurements of the light from the scene, and actual sRGB values in cameras. We measured these discrepancies. These modifications to scene information introduce large changes in spatial information and make computer vision algorithms less accurate. Camera firmware and software modify color separation data for better looking pictures. These modifications need to be removed for accurate scientific scene analysis. We describe a computer program that converts a RAW digital camera file to calibrated file, in which digit value is proportional to log scene radiances.

Introduction

Image capture is the first step in computer vision. Spatial information processing is key to many recognition problems. Face, object, motion, feature recognition, and high-dynamic range imaging begin with spatial scene information. It would be nice to assume that, when we open a digital camera file and read the RGB digital values of a pixel, we get calibrated radiance measurements of the light from the scene. Cameras are designed to make attractive pictures using many firmware algorithms. Optical limits and firmware image processing modify scene radiance information, thus altering the scene's spatial relationships in the captured image.

- High-end professional digital cameras modify the output Jpeg data to reduce the effects of optical vignetting and other optical artifacts. This approach uses specific camera and lens metadata to reduce known artifacts.
- The light on the camera image plane is scene radiance plus scene-dependent veiling glare [1]. Although veiling glare removal would be highly desirable, it is not possible [2].
- Spectral information is not accurately recorded in standard digital color separation data. The improvements in color photography from the use of color masking are found in most color film reproduction processes. The technique was introduce by Albert [3] in 1889.

Calibration of scene radiance vs. camera response is required for scientific use of color digital camera output.

If a proper calibration is done, is it possible to eliminate "engineered errors"? The primary question here is the size of the discrepancies between the scene's actual radiance measurements, and the digital rendition stored in the memory of the camera. After all, that stored image is the data that we use to analyze and manipulate images. The achromatic function of sRGB is not significantly different from Munsell Value. As well, color cameras show only small deviations from reproducing Munsell Value. However, the chromatic errors are quite large, much greater than we expected. Camera responses stored in memory are highly enhanced chroma renditions. These transformations make good-compromise scene renditions for most photographic subjects. However, these nonlinear chroma enhancements seriously distort the results of multiple exposure techniques to capture HDR scene information. We report on the size and nature of these departures from the sRGB scene measurements.

Although these departures from accurate scene rendition are well known to camera engineers [4-11, 27], there are many computer experiments in which the actual magnitude of these errors is larger than expected by their authors. These departures from accurate scene radiances can have significant adverse effects on image processing algorithms, such as:

- Object recognition
- Color balance from image statistics
- Retinex HDR processing

Figure 1 is a photograph of multiple objects with identical matte surfaces in nonuniform illumination. Sunlight is the only light source so that the spectral distribution of the illumination is constant.

Figure 1. Jpeg photograph of oranges, lemons and limes in sun and shadow.

The range of light in the scene slightly exceeds the range of the camera, however we have no difficulty identifying which fruits are oranges lemons and limes. In Figure 2 we manually selected 38 circular image segments. They are identified in Figure 2 top by magenta circles. These segments are shown on a uniform gray background in Figure 2 bottom. While the image segments appear to be normal lemons in Figure 1, we

can see that the range of camera responses to lemons varies from white to black in figure 2 (bottom).

In Figure 3 we manually selected 42 circular image segments. They are identified in Figure 3 (top) by blue circles. These segments are shown on a uniform gray background in Figure 3 (bottom). The response to oranges covers the entire camera range from white to black.

Figure 2 (top) Magenta circles show lemon segments; (bottom) segments viewed on a constant gray background.

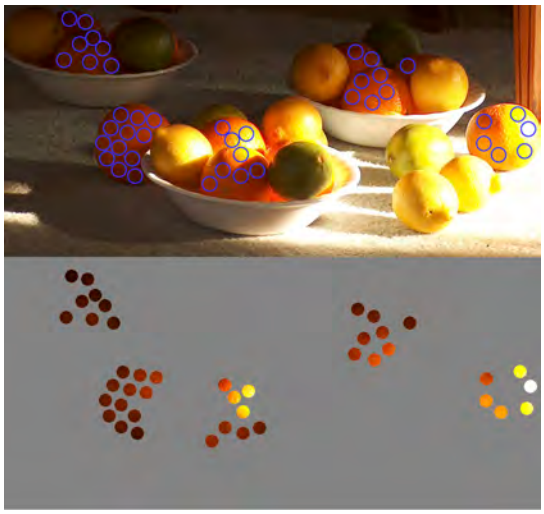

Figure 3 (top) Blue circles show orange segments; (bottom) segments viewed on a constant gray background.

We measured the average *R, G, B* camera digits for each lemon and orange image segment in a Jpeg image file. We wanted to compare the chromatic representation of the camera response to these constant objects. We used camera chromaticity values *(r,g)* using the formulae: *r = R/(R+G +B); g = G/(R+G+B),* with *R, G, B* equal to the pixel values taken for a particular color circle in the jpeg image file. These chromaticity values are specific to the camera system and file format. They should not be confused with colorimetric chromaticities *(x, y)* that represent camera independent transforms of *X,Y,Z*.

We plotted the *(r,g)* values of each segment in Figure 4. All possible colors fall in the lower triangle. The perimeter of the triangle describes the locus of maxima chroma with R at the bottom right, G at the top left, and B at the bottom left. The maximum possible yellow (Y) falls half way between R and G at *r = g* = 0.5. Over-exposure of a few segments resulted in plot points on the achromatic (0.33, 0.33) center. All other orange chromaticity values fall on the chroma limit line at 45°. They cover the range from Y to approach R. The lemon segments have some less than full chroma values, but overlap the orange segments with the exception of those near R. Clearly these *r, g* chromaticity values do not represent the surface of the objects. Clearly, they cannot be helpful to the evaluation of objects and scene characteristics, such as illumination. Constant object surfaces have highly variable digital signatures. The preferred rendering signal processing in this standard jpeg image file has transformed the spatial information from the scene. Constant surfaces in constant illumination spectra become highly variable chromaticities in bright light and shadows. In other words, standard camera renditions of scene colors change greatly in different amounts of light in the same scene under the same spectral illumination. Scientific image processing applications, such as object recognition and spatial HDR imaging, require accurate scene radiances. Attractive, but uncalibrated, images with "engineered errors" should be avoided.

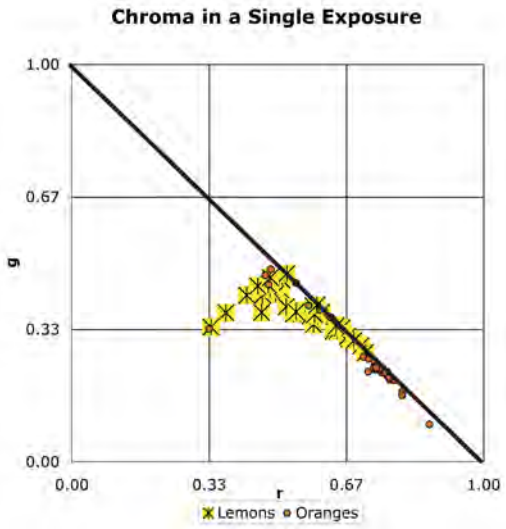

Figure 4 plots the chromaticities recorded by lemons and oranges.

As describe above, it is very well known in the camera engineering community that standard camera digital values are not accurate renditions of scene radiance. The problem is that the magnitude of the departures from accurate rendition is not generally understood.

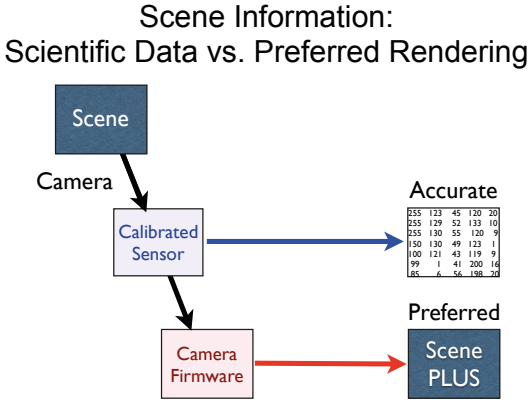

Figure 5 illustrates the choice between accurate scientific data and camera manufacturers' preferred rendering for more attractive pictures. Camera firmware modifies sensor response to render "Scene Plus" images, that contain "engineered errors" in their scene rendition.

Captured Scene Information

Figure 5 illustrates the choice we have in capturing scene information. Standard camera practice optimizes the appearance of the scene for its customers. It renders the preferred representation of the scene (Scene Plus), i.e. what most observers would consider "a better looking image". However, some scientific applications attempt to use digital cameras to capture actual RGB scene radiances in the visible spectrum.

Traditional Color Separations

Traditional color separation photographs are made with red (R), green (G) and blue (B) color filters on panchromatic black and white film. This technique was described by Maxwell in 1861 at the Royal Institution.[12] These three R, G, B photographs are records of the spectral information contained in the light from a scene. They approximate square band filters to isolate the long-, middle-, and short-wave portions of the visual spectrum.

Great care must be taken to insure that a scale made up of gray papers in the scene has equal optical densities in each R, G, B separation. Thus, whites, grays, and blacks will be achromatic in the color rendition. These black&white color separations record the relationship of the light from the scene.

Digital Color Separations

Digital color separations are available from any photograph by selecting R, G, B channels in applications, such as Photoshop® or ImageJ®. These digits for each pixel are the values stored in the file for the photograph. The stored color separation digits saved to memory are the output of a large number of image processing steps performed by the camera in firmware. A partial list includes: anti-blooming, noise suppression, sensor readout, digitization, high speed transfer, tone mapping, color balance, chroma boost, conversion to the color space expected by printers and displays. All these processes can introduce nonlinear transforms of the color space. Some of these nonlinear steps can be eliminated by analyzing RAW format images.

Measurements of Three Types of Color Separations

This paper measures the digital values of red (R), green (G), and blue (B) color separations, with variable exposures, in three different types of images:

1. Traditional panchromatic black and white film separations using Wratten 25, 58 and 47B filters, then digitized.
2. Standard jpeg images from a commercial camera.
3. Black and white RAW images made on the same camera. We acquired the partially processed RAW camera data, using the “LibRaw” Image Decoder Library[13]. This is a black and white image with the mosaic pattern. We converted this mosaic image with calibration data into linear RGB data, that we called "RAW* separations”. These RAW* RGB values are the color information part-way through the firmware system. It reports the data before the demosaic, color balance, chroma boost, tone scale, color management and compression.

Maxwell's film separations

We made a series of exposures (variable EVs) of the Munsell ColorChecker® in sunlight. We used Fuji ACROS 100 film [14] in a 35mm camera. We used variable exposure values (EVs) similar to those in HDR scene capture. Film with linear calibration of the scanner should give constant reports for constant object surfaces in the scene. We developed the black and white film negative images and scanned the range of exposures mounted as a set on the scanner, in the style of a proof sheet. By having all negatives in the same scan. We prevented individual image processing of the different negatives. We measured the red, green, blue scanned digits (RGB) for the gray scale at the bottom and the BLUE, GREEN, RED, YELLOW, MAGENTA, CYAN ColorChecker® squares above them using ImageJ® to calculate an average response for each square. We applied a calibration LUT to each film average to convert film-scan digit to linear scene radiance (*R, G, B*). We calculated *(r,g)* chromaticities from *R, G, B*. using the formulae: $r = R/(R+G+B)$; $g = G/(R+G+B)$.

The film data (Fig.6, left) included a calibration LUT to convert scanner digits to linear scene radiance values. The plot includes the chromaticities of *R, G, B* triplets that were free from scanner saturation at max and min. These plots of the papers' chromaticities, with varying exposure, superimpose on each other. The calibrated film process records a unique *(r,g)* chromaticity for each color paper, regardless of exposure.

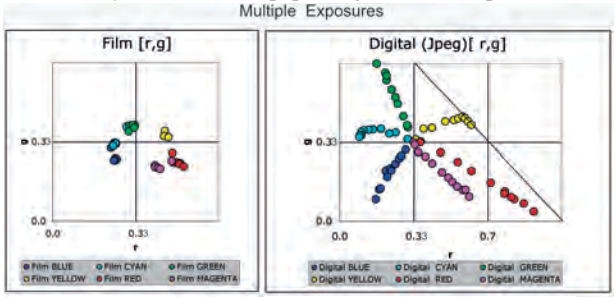

Figure 6. Chromaticities of ColorChecker® squares in variable exposures. (left) plots the film color separation method; (right) plots standard Jpeg digital images. Each color point is the plot for different exposures (EVs) of the same scene color square.

Digital camera color separations (jpeg)

We repeated the variable exposure values (EVs) similar to film. We used a Panasonic DMC-G2K micro4/3 camera [15] for both Jpeg and RAW images. The digital ranges of the RGB Jpeg values for a single exposure were comparable to those from the scan of the black and white films. The achromatic range of digits from film and jpeg representations of the scenes were comparable. The two sets of color separations varied considerably in their chromatic responses. The recorded chromaticity value for a colored square is influenced by many camera firmware processes, such as tone scale, color balance, color enhancement, color management. These nonlinear processes can have variable influence on the chromaticities they record. Extreme over- and under-exposures have saturated white and black responses with neutral chromaticity values [0.33, 0.33]. Exposures that move the colored square's response up and down the nonlinear tone scale influence the chromaticity values of colored objects. We expected slightly different results for digital cameras because of nonlinear color processing. The images captured here represent standard color photographs used by most camera owners. We made variable exposures of the Munsell ColorChecker in sunlight. The results of standard digital photographs (Jpeg) show that color information varies considerably with exposure (Fig.6, right). While black and white film data gave constant chromaticity values for a given color paper, the digital *r,g* varied over the entire possible range of chromaticities, just by varying exposure.

Calibration of scene radiance vs. camera response is required for scientific use of color digital cameras. Figure 7 expands the details outlined in Figure 5.

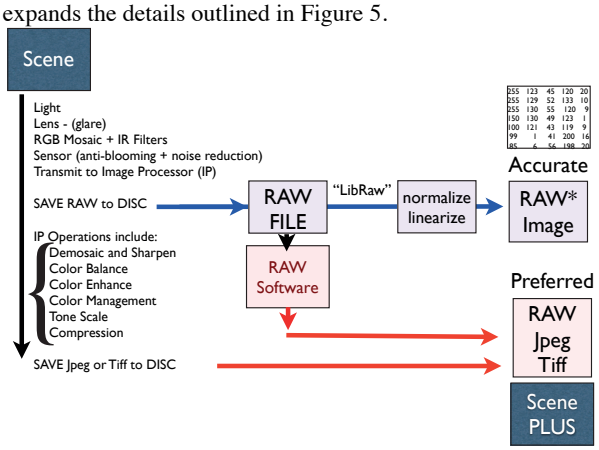

Figure 7. Accurate scientific data and camera manufacturer's preferred rendering use different pipelines. Camera firmware modifies sensor response to render "Scene Plus" images, that contain "engineered errors". Scientific data can be measured using RAW images with calibration steps (linearization and normalization) to make RAW data.*

Standard color files (jpeg, or tiff) and commercial RAW processing software introduce large modifications to the color records. Taking photos in RAW format has become a trend in photography. There is the notion that this format preserves the scene information better than standard formats. However, this can only be true for specially calibrated RAW image data. If standard RAW rendering software applies similar non-linear algorithms for color processing, then the problem persists. As a result, the unwanted nonlinearities have now been introduced to the image data by the RAW rendering software, instead of the camera engine. These modifications of scene data are of value to the manufacturer, because it sells cameras. However, it introduces calibration challenges for scientists who want to use camera data as captured scene radiances. They cannot without additional camera calibration.

The multiple-exposure film data superimpose in Figure 6 (left) because the calibrated film digits are linear transforms of scene radiances. The film has a long linear range of sensitivities between maxima and minima over three log units. The nonlinearities in the film scanner were removed by the calibration *R, G, B* LUTs.

Color enhancement using films have been in use for more than a century [3, 14-16]. One example combines an unsharp short-wave negative mask with a long-wave positive film, along with similar negative masks for the other separations. The superposition of the color separation films with its complementary mask make a lower-contrast rendition for grays and a higher-chroma rendition for colored objects. This increase in chroma modifies the edges and spatial information recorded from the scene,

In digital systems scene chroma can be distorted by nonlinearities in signal processing. To correct this we made digital images that accurately record scene information. We made an exposure series covering a range of exposures of 30 to 1. We used the same Panasonic DMC-G2K micro 4/3camera [13] for both Jpeg and RAW images.(Figure 8).

We used the "LibRaw" Image Decoder Library [11], built on "dcraw" library, which has also been used in the Funt HDR dataset [17] and Natural Image database [18]. More specifically, we used the "unprocessed" function of LibRaw, which outputs the unprocessed data of the RAW file, without applying any processing such as demosaicing, white balance, gamma modification, image enhancement, or compression.

This results in an image in which the Bayer pattern is visible (Fig. 8, bottom). The R, G and B digital responses to the Bayer pattern filters are different, and the RAW data are not normalized. This is clearly depicted in the histogram of the white square of the ColorChecker, where, every sensor has a different intensity value for white. For this reason, we used R, G, B calibration LUTs to scale the sensor responses. The LUTs should remove any Tone-Scale nonlinearities, and have the same output response for achromatic patches. We use the name RAW* to describe the output of this process that independently linearizes, and then normalizes the so called "unprocessed" RAW data.

Figure 8 (top) JPEG. (bottom) RAW files from same exposure.

The results in Figure 9 show that the RAW* color separation chromaticities are more like the traditional ones from film. RAW* color separation data, with linear calibration, exhibit more constant chromaticities with varying exposures.

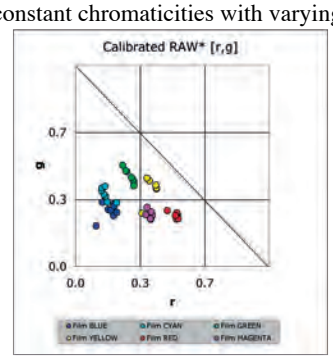

Figure 9. RAW Chromaticities of the ColorChecker® squares in variable exposures. Each color point is the plot for different exposures of color papers using RAW* color separation values with linear calibration.*

Nonlinear color modifies spatial content

Many scientific applications benefit from the ability to capture scene information using digital cameras. Examples include measuring scene radiances, material recognition, and spatial image processing. We saw an accurate rendition of the spatial information in traditional film separations in each waveband. However, standard digital color processing changes that spatial information. High-chroma colors have the largest "engineered errors". Figure 10 (top) illustrates a synthetic image with colored areas having near maximum chromas made of digits 70 and 225.

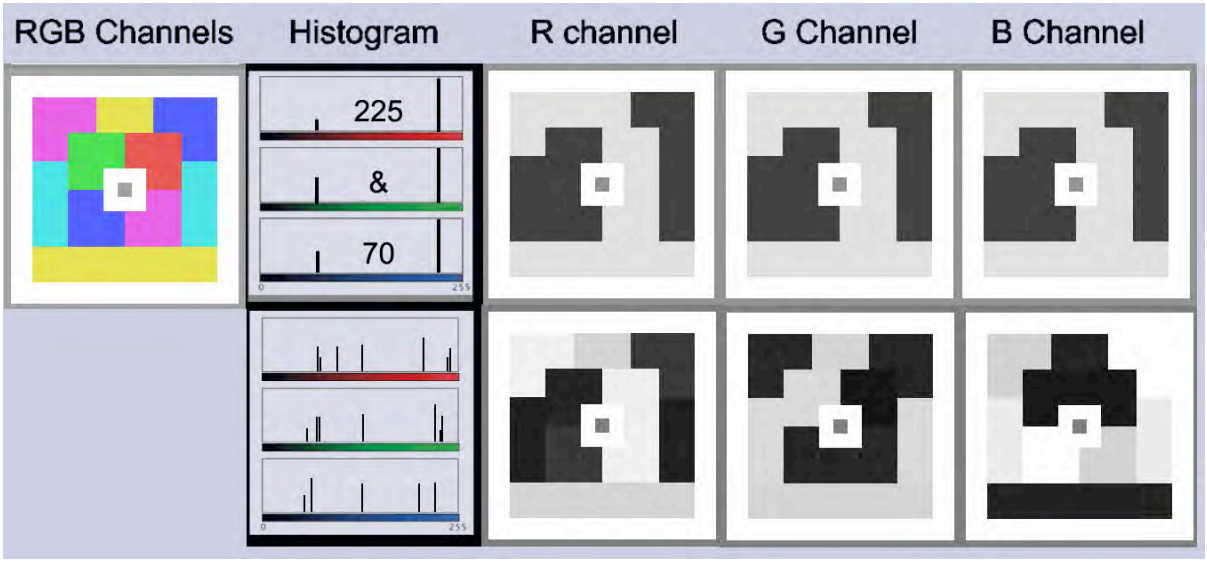

Figure 10 shows a synthetic color image, its histograms and separations. It illustrates the spatial effects of "engineered errors". The colors in the top row separations are made up of digital values 70 and 225. The bottom row shows standard color camera processing of the middle-row image. Its histograms shows the color changes. The R, G, B color separations show that the spatial content of the scene has been changed.

These colors in the top row synthetic separations have only values 225 and 70 [(R=225,70,70; Y=(225,225,70); G=(270,225,70); C=(70,225,225); B=(70,70,225); and M=(225,70,225)]. Using the measurements described above for scene and jpeg renditions we transformed the synthetic image in the middle row to make the bottom row. Standard color digital processing renders the bottom row of color separations. Note that the distribution of histogram values has changed. The spatial content of the RGB images has also changed. Accurate spatial content is critical for many computer vision applications. They include HDR reproduction and spatial image processing in sun and shade.

Digital cameras as linear sensors

The form of the chromaticity equations (*r = R/(R+G+B); g = G/(R+G+B),* requires truly linear *RGB* input data. Even small departures from linearity will make identical color surface have variable chromaticity values. We all know that silicon sensors have a linear response to scene radiance. Nevertheless, we cannot project that linearity onto assumptions about camera response. We also need to be certain that camera performance is linear over the entire dynamic range of the camera.

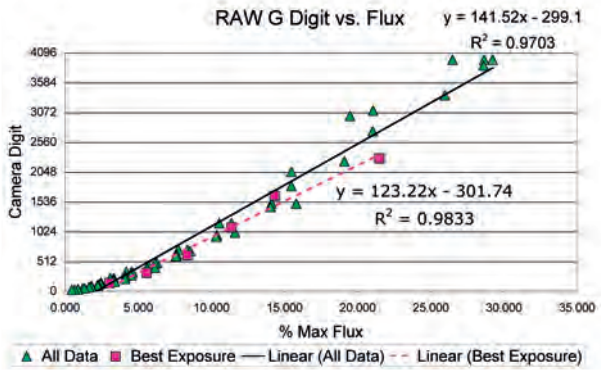

Figure 11. Plot of Raw G camera digits vs. scene flux. Magenta squares plot the data from the best exposure; green triangles plot data from all exposures. The best fit for all data has 15% higher slope and poorer fit than that of the best exposure.

Figure 11 plots the RAW G digit values vs. relative scene flux for the series of 12 different exposures of the 6 white, gray black squares in the ColorChecker. The magenta squares plot the six digital values of gray squares from the best exposure. The linear least-square-fit for the best exposure has a slope of 122.32 (R^2=0.983). In analyzing the data from all grays, we removed data from saturated maxima and minima values. We plotted all other data for all 12 exposures and found a different linear fit with slope of 141.52, with poorer fit (R^2=0.970).

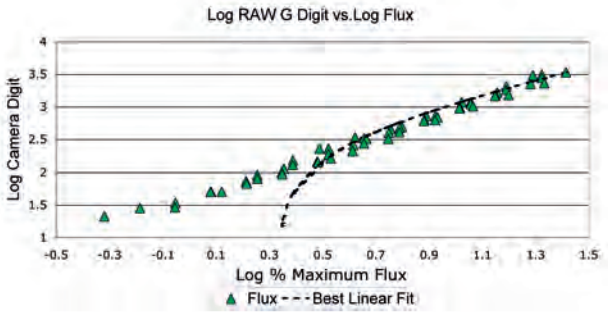

Figure 12 replots the data in Figure 11 using log log axes. The lower half of the logarithmic range departs from the linear fit. The upper half falls slightly below the linear fit.

We replotted the 12 exposure data using a log log scale to be able to see the cameras response in both high and low exposure regions.

The linear equation [y=141.52x-299.1] plots as a logarithmic shape connecting black squares on log log axes. The linear fit curve in the top half of the camera's dynamic range (0.5 to 1.5) is slightly above the measurements. The linear fit does not represent the bottom half of the camera's dynamic range (-0.5 to 0.5). This section of the plot has 18 data points. Six of them are measurements of the black area in the ColorChecker. Four points are from the dark-gray square measurements (Gray 4). That suggests that camera veiling glare may be a part of the problem.[1] However, the Gray1 area has 2 data points above the linear fit line; Gray2 and Gray3 areas have 3 each. These points indicate that the shape of the camera response function in this region is not caused by

scattered light alone. As well, all camera digit values below 256 did not fit the linear response function. While the range from 0 to 256 is only 1/16th the range of digits of 0 to 4096, it represents half of the camera's RAW dynamic range.

Program: RAW2RAW*

We used the techniques and the calibration data described above to develop a software program that converts RAW format images, available from many of today's commercial cameras, into the proposed RAW* image format. The main objective of this format is to describe better the radiance of the scene, rather than exhibit good-looking images. This "RAW2RAW*" file conversion software employs the engine of the "LibRaw" Image Decoder Library [13], which is based on the "dcraw" library. All the settings of LibRaw have been selected so as to ensure that the raw image data will not be affected by the usual rendering that the camera firmware applies. For a similar reason we selected the Portable Pixel Map (PPM) image file format, over other classic file formats (e.g. TIFF or BMP), as a container for the RAW* data, since PPM is the simplest and ensures that no compression or any other transformation is applied to the data. [21]

The RAW* format is an array of digits that are proportional to log scene radiance as captured by the RGB filters in a camera. It is the triplet of radiances integrated by the silicon spectral sensitivity as modified by the R, G, B filters. These values are influenced by the signal processing components on the sensor and transport mechanisms prior to the storage of RAW file data.[22] In other words, it makes use of the RAW camera data, before nonlinear camera firmware rendering algorithms are applied. The current algorithm does not demosaic the image, so the size of the original image is reduced from 4016 × 3016 to 2008 × 1580 pixels. We averaged double green pixels as described by Funt's HDR dataset[19]. The RAW2RAW* conversion software also used three one-dimensional LUTs (RLUT, GLUT, BLUT) to convert the 12-bit camera pixel values to relative log radiance values. We used the camera response RGB digits from the multiple exposures from the white-gray-black squares in the bottom row of the ColorChecker. The LUTs convert camera digits to relative scene flux that is the product of measured scene reflectance and camera exposure time. These linear scene flux are scaled to adjust for the spectral content of the illumination. The scaling makes the achromatic ColorChecker® squares have equal RGB output values. The maximum values of the LUT outputs is the highest flux values below the saturation of the G camera response. We fabricated the LUTs using 8-bit data and the program interpolates them to 16-bits for processing and export of the RAW* files.

Figure 13 shows an example of the three RAW* separation images and their histograms.

Fig 13. RGB calibrated separation images of RAW file with histograms.*

Fig. 14 compares the RAW unprocessed data from the black and white "LibRaw" library; JPEG image,: the combined RGB RAW data; and the RAW* output of the RAW2RAW* software.

.Figure 14. Examples of RAW unprocessed B&W, JPEG image, combined RGB RAW data ,and the RAW output of the RAW2RAW* software.*

Notice that the images in the lower half of Fig. 14 are half the size of the original unprocessed raw data, due to the lack of demosaicing. The combined RGB raw image (lower left corner of Fig. 14), depicts the unnormalized and non-linear data, used directly from the RAW image data (upper left corner of Fig. 14). Since G has greater sensitivity the Combined RGB RAW image appears green. When applying the processing techniques, described earlier in this paper, to the Combined RGB raw image, the result is the RAW* image (lower right corner of Fig. 14). The RAW* image has lower contrast and color saturation compared to the JPEG image, since no chroma boost, tone scale gamma correction and color management are applied. However, one should keep in mind that the best looking image is not the objective of the proposed software, but rather, a better representation of the scene RGB radiances. The RAW* digits are proportional to log scene radiances measured from the scene. They are scaled so that white gray and black papers have equal digit values.

Figure 15 plots the *(r,g)* chromaticities from the RAW* image. We took the antilog of image data to get linear *RGB* values.

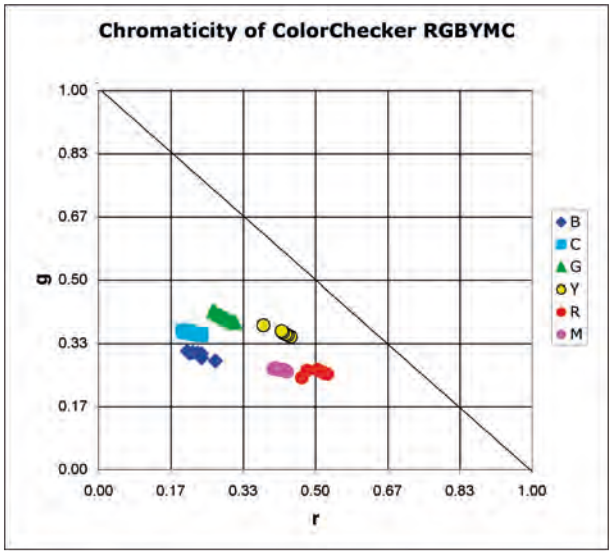

Figure 15. Chromaticities of the ColorChecker® squares in variable exposures from RAW images made by RAW2RAW* program.*

The RAW2RAW*program reads in a RAW image. It also reads in the specific calibration RGB LUTS for the scene. These LUTS are specific to the:

- camera sensitivity and pre RAW file processing,
- spectral content of the illumination,
- scene-dependent veiling glare in the image on the sensor.

Although it would be very desirable to have a camera calibration for all scenes and all illuminations, that is not possible. Accurate scene renditions will not help to sell cameras. It will help considerably in any computer algorithm that makes spatial comparisons.

The RAW2RAW* conversion software, is available for public use and can be freely downloaded from:

http://www.https://sites.google.com/site/vonikakis/research/raw

Discussion

The sensible way to calibrate a camera is to photograph a color test target.[23-27] Many targets have a range that covers the range of reflectances in paints and objects surfaces. As well, the sensible thing to do is to use illumination that is uniform across the test target in both irradiance and spectral content. Surfaces have a measured range of reflection of about 30:1. The camera response range we measured above was about 60:1. The camera range was twice the test target range, so calibration in uniform illumination works well.

This actual measured radiance range for this scene seems small compared to the range of digital values, in this case 12 bit data (4096:1), that represent the scene. The measurements of this camera's ability to capture range accurately is in good agreement with other camera measurements. For example, the usable range for a Nikon Coolpix 990 camera is 40:1 (1.6 log units) using a target with a white surround. When the white surround is replaced with opaque glare-free black the range jumps to 631:1 (2.8 log units).[1]

The interesting problem in scene photography is that uniform illumination (irradiance and spectra) is extremely rare. With the exception of photographs made on beaches, most scenes have highly nonuniform illumination. Image processing of real scenes require accurate scene information that far exceeds the range of most color calibration measurements. It is safe to assume that the camera response is linear for a well exposed test target (Figure 11). But, as we saw in Figure 12, the response of our camera was nonlinear for the bottom half of its range. These results point out the importance of calibration over the entire range of camera response when using camera image files as input to image processing algorithms. As long as the scenes used in image processing are restricted to the range of test targets in uniform illumination, then camera images are reasonable input data for computer vision algorithms. However, if the scene content include nonuniform illumination, then much more specific measurements of camera response functions are needed.

The success of commercial digital photography requires a partnership with the human visual system. Vision's spatial processing, that leads to color constancy, solves these nonuniform illumination problems when we look at images. Visual appearance is a very unreliable way to measure radiance. Looking at images is an unreliable assessment of quantitative image processing. Unfortunately, when we attempt to measure the light in images, the input to vision, we find just how difficult a problem it is to capture accurate scene information.

Summary

Standard camera firmware and software modify color separation data for better looking pictures. These modifications need to be removed for accurate scientific scene analysis. Spatial image processing is distorted by these "engineered errors". Nonlinear tone scale functions, as well as color enhancement algorithms distort the color information captured from the scene. The magnitude of these distortions is very large. We describe a calibration process and a computer program that can remove some of these "engineered errors" using scene-specific calibration.

Acknowledgements

The authors want to thank Alessandro Rizzi, Geoff Wolfe Ricardo Motta, Francisco Imai, Chris Cox, Tom Lianza, and Mary McCann for helpful discussions.

References

[1] McCann JJ, Rizzi A, The Art and Science of HDR Imaging: Chapter 11, John Wiley & Sons, Chichester, (2012).

[2] ISO 9358: 1994 Standard, Optics and Optical Instrument: Veiling Glare of Image Forming Systems. Definitions and Methods of Measurement. International Organization for Standardization, Geneva, (1994).

[3] Albert E, German Patent, 101379, (1989).

[4] Adams, J.; Parulski, K.; Spaulding, K.; "Color processing in digital cameras", IEEE Micro, 18:6, (1998).

[5] http://www.color.org/index.xalter

[6] Spaulding KE, Woolfe GJ & Giorgianni EJ, "Image States and Standard Color Encodings (RIMM/ROMM RGB)", Proc. IS&T Color Imaging Conf, 8, 288-294, (2000).

[7] Woolfe GJ, Spaulding KE, & Giorgianni EJ, "Hue Preservation in Rendering Operations–An Evaluation of RGB Color Encodings", Proc. IS&T Color Imaging Conf, 10, 317-324, (2002).

[8] Holm J, Tastl I, Hanlon L, & Hubel P, "Color processing for digital photography", in Colour Engineering: Achieving Device Independent Colour, Green P. & MacDonald L., eds., Wiley, (2002).

[9] ISO 22028-l:2004, "Photography and graphic technology: Extended colour encodings for digital image storage, manipulation and interchange; Part 1 Architecture and requirements, Annex C, Section C12, p 45, (2004).

[10] Holm J, "Color processing for digital cameras", SPIE Electronic Imaging Newsletter, 14.1, January (2004).

[11] Ramanath, R.; Snyder, W.E.; Yoo, Y.; Drew, M.S.; "Color image processing pipeline", IEEE Signal Processing Magazine, 22 Issue:1, (2005).

[12] Maxwell J.C. *The Scientific Papers of James Clerk Maxwell*, ed. Niven, New York: Dover 410–44, (1965).

[13] "LibRaw" Image Decoder Library <www.libraw.org/>

[14] <www.fujifilmusa.com/products/profesional_photography/film/neopan_black_white/100_acros/index.html>

[15] Panasonic DMC-G2K http://service.us.panasonic.com/OPERMANPDF/DMC2K.PDF\

[16] Friedman J.S. (1944) Chapter 19, Masking, in History of Color Photography, The American Photo Publishing Co, Boston, 273-295, (1944).

[17] Spencer D.A., Chapter XIV Masking and Colour Correction, in Colour Photography in Practice, The Focal Press, London, 297-328, (1966).

[18] Yule, J A C, Colour Reproduction in the Graphic Arts, in Color Photography, in Neblette's Handbook of Photography and Reprography, Materials Processes and Systems, 7th ed., Sturge J, Van Nostrand Reinhold, New York, 466-480, (1977).

[19] http://www.cs.sfu.ca/~colour/data/funt_hdr/

[20] http://www.cps.utexas.edu/natural_scenes/db.shtml

[21] http://netpbm.sourceforge.net/doc/ppm.html

[22] Bouman K, Ramachandra V, Atanassov K, Aleksic M, and Goma SR, "RAW camera DPCM compression performance analysis", Proc. IS&T/SPIE Electronic Imaging Conf.,7867, 7867ON1-7, (2011).

[23] McCamy C, Marcus H, & J. Davidson J, "A color rendition chart", Journal of Applied Photographic Engineering, 2, 95–99, (1976).

[24] Abdulwahab M, Burkhardt J & McCann JJ, "Method and Apparatus for Transforming Color Image Data on the Basis of an Isotropic Colorimetric Space", US Patent 4,839,721, (1989).

[25] Johnson T, "Methods for characterizing colour scanners and digital cameras" Displays, 16, 183–191 (1996).

[26] Barnard K & Funt B, "Camera characterization for color research", Color Research and Applications, 27, 153–164, 2002.

[27] Green P ed. *Color Management Understanding and Using ICC Profiles*, Wiley/IS&T, Chichester, (2010).

Author Biography

John McCann received a degree in Biology from Harvard College in 1964. He worked in, and managed, the Vision Research Laboratory at Polaroid from 1961 to 1996. He has studied human color vision, digital image processing, large format instant photography, and the reproduction of fine art. His publications and patents have studied Retinex theory, color constancy, color from rod/cone interactions at low light levels, appearance with scattered light, and HDR imaging. He is a Fellow of the IS&T and the Optical Society of America (OSA). He is a past President of IS&T and the Artists Foundation, Boston. He is the IS&T/OSA 2002 Edwin H. Land Medalist, and IS&T 2005 Honorary Member.

Vassilios Vonikakis received the diploma and PhD in Electrical and Computer Engineering from the Democritus University of Thrace, Greece, in 2002 and 2008 respectively. His research interests include vision, HDR imaging, and computational photography. He has previously worked as a researcher for the University of Rome "La Sapienza". He currently is a Post-Doctoral fellow in the Advanced Digital Sciences Center (ADSC), Singapore, which is a part of the University of Illinois at Urbana-Champaign.